Available online at www.sciencedirect.com
SCIENCE DIRECT®
Journal of Sound and Vibration 288 (2005) 215–234
JOURNAL OF SOUND AND VIBRATION
www.elsevier.com/locate/jsvi

Structural system identification in time domain using measured acceleration

Joo Sung Kang[a], Seung-Keun Park[a], Soobong Shin[b], Hae Sung Lee[a,*]

[a]*Department of Civil Engineering, Seoul National University, Seoul, Republic of Korea*
[b]*Department of Civil Engineering, Inha University, Incheon, Republic of Korea*

Received 2 February 2004; received in revised form 23 April 2004; accepted 4 January 2005
Available online 10 May 2005

Abstract

This paper presents a system identification scheme in time domain to estimate stiffness and damping parameters of a structure using measured acceleration. An error function is defined as the time integral of the least-squared errors between measured accelerations and calculated accelerations by a numerical model of a structure. To alleviate the ill-posedness of SI problems a regularization technique is employed and a new regularization function for the time-domain SI is proposed. The regularization factor is determined by the geometric mean scheme. The validity of the proposed method is demonstrated by a numerical simulation study on a two-span truss bridge and by an experimental laboratory study on a three-story shear building model.

1. Introduction

Various system identification (SI) schemes have been developed to verify structural models or to assess damage in a structure during last few decades. Based on the types of measured response, SI algorithms can be classified by static SI [1–4], frequency-domain SI [5–7], and time-domain SI [8–11]. Since it is difficult to measure static displacements of actual structures, frequency-domain

*Corresponding author. Tel.: +82 2 880 8388; fax: +82 2 887 0349.
E-mail address: chslee@plaza.snu.ac.kr (H.S. Lee).

0022-460X/$ - see front matter © 2005 Elsevier Ltd. All rights reserved.
doi:10.1016/j.jsv.2005.01.041

SI or time-domain SI may be more practical in real applications. Even if frequency-domain SI algorithms utilize the same source of dynamic responses as time-domain SI, the amount of data dealt with is remarkably reduced through transformation. Due to the ease in handling data, frequency-domain SI algorithms have been more widely developed and applied. However, local damage may influence higher modes that are usually difficult to measure from experiments [12]. Moreover, damping properties of structures cannot be estimated in frequency-domain SI. To overcome these drawbacks of the frequency-domain SI and to yield more meaningful identification results, the time-domain SI schemes are an attractive alternative.

In developing a time-domain SI algorithm, the incomplete measurements in space and state should be considered in addition to measurement noise [8]. The incompleteness in space occurs when structural responses are not measured at all degrees-of-freedom (dof) corresponding to its numerical model. Some SI algorithms circumvent this difficulty by including the unmeasured dof as system parameters to be estimated in SI [8]. The incompleteness in state also occurs in most dynamic measurements because only one state of acceleration, velocity, or displacement time history is usually measured. Numerical schemes for integrating or differentiating the measured state vector [8] are applied to compute unmeasured state vectors. Since the numerical schemes naturally develop computational error and amplify noise in measured responses, the most desirable way may be to avoid computing unmeasured responses using measured data in formulating a SI algorithm.

This paper presents a new time-domain SI algorithm using an output error estimator based on acceleration. The proposed SI algorithm estimates structural parameters through the minimization of an error function defined by the time integral of the least-squared error between the measured and the calculated accelerations. Since the error function is defined only with the time history of acceleration measured at limited locations, the algorithm does not require any information on actual dynamic responses other than acceleration.

It is well known that a SI problem is a type of ill-posed problem [13,14], which suffers from severe instabilities caused by noise and incompleteness in measurement. The instabilities are characterized as non-existence, non-uniqueness and discontinuity of solutions. To alleviate the ill-posedness of SI problems, the regularization technique has been widely employed for various engineering problems [2–4,13,14]. In the regularization technique an additional constraint on system parameters, which is referred to as a regularization function, is imposed to the original minimization problem defined by the error function. It is very important to define a proper regularization function that is able to describe characteristics of a SI problem in hand [2–4,14]. This paper proposes a new regularization function for time-domain SI defined as the time integral of the squared first time derivative of system parameters. The geometric mean scheme (GMS) [4] is utilized throughout the study to determine the regularization factor multiplied to the regularization function.

It is assumed that mass is known a priori and structures behave linearly. Since structural dynamic behaviors are not only dependent on mass and stiffness but also on damping properties, estimation of damping parameters may be important for correct identification of structural systems. Nevertheless, most time-domain SI schemes have assumed damping as known and thus dealt solely with stiffness parameters [9,10]. In the paper, the structural damping is modeled by the Rayleigh damping [15], and two Rayleigh damping coefficients are estimated together with the unknown stiffness parameters.

To validate the proposed method, a numerical simulation study on a two-span truss bridge and an experimental laboratory study on a three-story shear building are carried out. Damage is simulated as the reduction in axial rigidities of a few members for the simulation study while damage is implemented by loosening the bolts at joints for the experimental study. To examine the developed algorithm with noisy measured data, random noise is added to the generated time history of acceleration in the simulation study. Discussions on numerical results and behaviors of the proposed method are presented.

2. Parameter estimation in time domain

2.1. Error function in time domain

The equation of linear vibrational motion of a structure can be expressed by

$$\mathbf{M}\mathbf{a}(t) + \mathbf{C}(\mathbf{x})\mathbf{v}(t) + \mathbf{K}(\mathbf{x})\mathbf{u}(t) = \mathbf{p}(t), \tag{1}$$

where **M**, **C**, **K**, **p** and **x** are mass, damping, stiffness matrix of a structure, load vector and the system parameter vector, respectively. Acceleration, velocity and displacement vector of a structure are denoted as **a**, **v** and **u**, respectively, in Eq. (1). The system parameters include stiffness and damping properties of a structure, which need to be identified.

In the formulation, it is assumed that mass properties, load history and the initial conditions for Eq. (1) are known a priori, and that the system parameters are invariant in time. The unknown system parameters are identified through the following minimization of the least-squared error between calculated and measured accelerations at observation points from the beginning up to current time τ.

$$\underset{\mathbf{x}}{\text{Min}}\ \Pi(\mathbf{x}, \tau) = \frac{1}{2}\int_0^{\tau} \|\tilde{\mathbf{a}}(\mathbf{x}, t) - \bar{\mathbf{a}}(t)\|^2 \, \mathrm{d}t \quad \text{subject to } \mathbf{r}(\mathbf{x}) \leqslant 0, \tag{2}$$

where $\tilde{\mathbf{a}}$, $\bar{\mathbf{a}}$ and **r** are the calculated and the measured acceleration at observation points and constraint vector, respectively. The notation $\|\cdot\|$ represents the Euclidean norm of a vector.

The parameter estimation method defined by a minimization problem as (2) is a type of ill-posed inverse problem, which suffers from instabilities such as non-existence, non-uniqueness and discontinuity of solutions [13,14]. The instabilities are triggered when measured data are incomplete and polluted by noise. Because of the instabilities, the minimization problem given in Eq. (2) may yield meaningless solutions or diverge in optimization process [4]. The regularization technique [2–4,13,14] is considered to be a rigorous way to overcome the ill-posedness of inverse problems. In the regularization technique, the original objective function is modified by adding a positive definite regularization function [2–4]. For a successful SI, a proper regularization function, which clearly defines characteristics of problems, should be selected.

2.2. Regularization function

As the system parameters are assumed to be invariant in time, the minimization problem (2) is supposed to yield the same results at any τ in case the measured accelerations are complete and

noiseless. However, the measured data are usually incomplete and polluted by various kinds of noise. Furthermore, the amount of measured data used in the SI varies with τ. Due to the aforementioned facts, the minimization problem (2) yields different system parameters for different time τ as illustrated in Fig. 1(a). That is, the system parameters are constant in the interval of $0<t\leqslant\tau$ for the fixed τ, but the constant values of the system parameters vary for different τ. Fig. 1(b) shows a schematic plot of a system parameter identified at different τ drawn against time.

In case the time-invariant assumption for the system parameters cannot be satisfied exactly by the nature of the problem, the magnitude of the time variance of system parameters should be reduced as much as possible by imposing the following minimization problem.

$$\underset{\mathbf{x}}{\text{Min}}\ \Pi_R = \frac{1}{2}\int_0^{\tau}\left\|\frac{\mathrm{d}\mathbf{x}(t)}{\mathrm{d}t}\right\|^2 \mathrm{d}t. \tag{3}$$

Here, $\mathbf{x}(t)$ denotes the system parameters identified by using the measured accelerations from the initial time 0 to time t as shown in Fig. 1(a). The minimization problem (3) may be considered as a weak constraint or a penalty function to impose the time-invariant assumption of the system parameters. The integral expression of Eq. (3) defines total change of the system parameters up to the current time. The objective function Π_R defined in Eq. (3) is used as the regularization function for time-domain SI.

A modified minimization problem with the regularization function (3) for the time-domain SI is defined as follows:

$$\underset{\mathbf{x}(\tau)}{\text{Min}}\ \Pi(\mathbf{x}(\tau),\tau) = \frac{1}{2}\int_0^{\tau}\|\tilde{\mathbf{a}}(\mathbf{x}(\tau),t)-\bar{\mathbf{a}}(t)\|^2\,\mathrm{d}t + \frac{\lambda^2}{2}\int_0^{\tau}\left\|\frac{\mathrm{d}\mathbf{x}(t)}{\mathrm{d}t}\right\|^2\mathrm{d}t \quad \text{subject to } r(\mathbf{x})\leqslant 0, \tag{4}$$

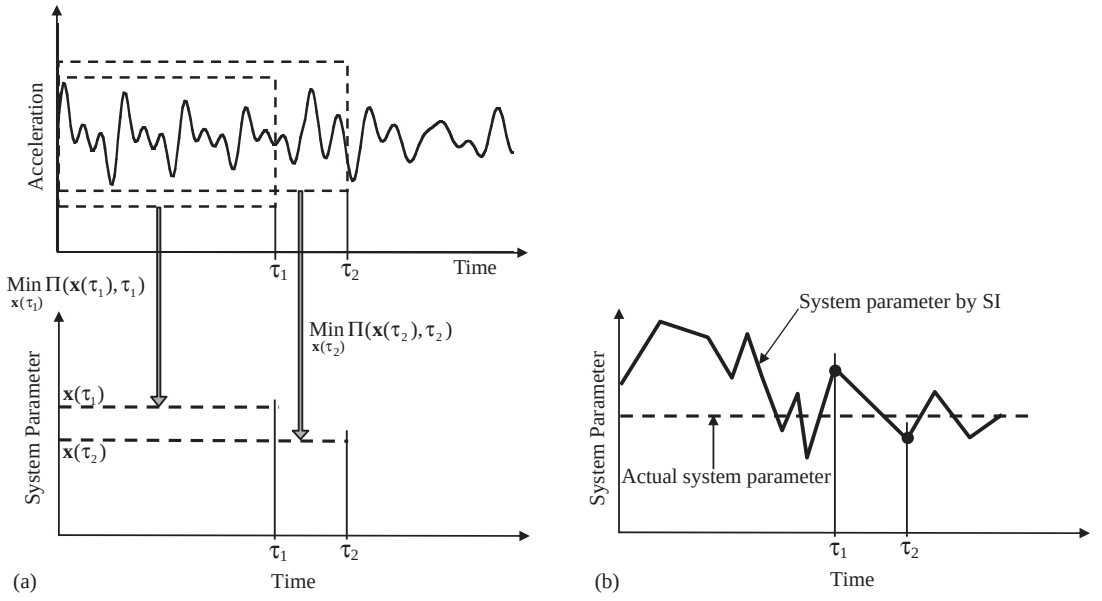

Fig. 1. (a) Time-domain SI at two different times. (b) Variation of a system parameter in time.

where λ is the regularization factor. Notice that the system parameters in Eq. (4) depend upon current time τ. The regularization effect in parameter estimation is controlled by the magnitude of the regularization factor. The regularization effect diminishes for a small regularization factor while the regularization function dominates for a large regularization factor [2–4]. In either case, the minimization problem (4) is unable to find meaningful system parameters due to instabilities or dominant regularization effects on the system parameters. Therefore, the selection of a proper regularization factor is very critical for the stability and accuracy of the solution of Eq. (4). The optimal regularization factor is determined by the geometric mean scheme (GMS) proposed by Park et al. [4]. In the GMS, the optimal regularization factor is defined as the geometric mean between the largest and the smallest non-zero singular value [16] of the Hessian matrix of the discretized error function, which is presented in the next section. The numerical rank [16] should be considered to determine the smallest non-zero singular value.

2.3. Damping model

It is difficult to model damping properties of real structures, and available damping models may be simple approximations of actual phenomena [15]. In most previous studies on the parameter estimation, damping properties of a structure are assumed as known, and thus only stiffness properties are identified [9,10]. Since damping plays an important role in structural dynamic responses, the damping properties should be considered properly in parameter estimation.

Among various classical damping models, the modal damping and the Rayleigh damping are most frequently adopted to model the structural damping. In the modal damping, a damping matrix is constructed by modal damping ratios, modal frequencies and mode shapes.

$$\mathbf{C} = \mathbf{M}\left(\sum_{k=1}^{N_d} 2\zeta_k \omega_k \boldsymbol{\phi}_k \boldsymbol{\phi}_k^T\right)\mathbf{M}, \tag{5}$$

where ζ_k, ω_k and $\boldsymbol{\phi}_k$ are the modal damping ratio, natural frequency and mode shape normalized to the mass matrix of the kth mode, respectively. In Rayleigh damping, a damping matrix is represented by a linear combination of the mass matrix and stiffness matrix.

$$\mathbf{C} = a_0\mathbf{M} + a_1\mathbf{K}, \tag{6}$$

where a_0 and a_1 are the Rayleigh damping coefficients. In case the Rayleigh damping is employed, the modal damping ratios are obtained as follows by equating (5) and (6).

$$\zeta_k = \frac{1}{2\omega_k}\,\boldsymbol{\phi}_k^T(a_0\mathbf{M} + a_1\mathbf{K})\boldsymbol{\phi}_k. \tag{7}$$

Because neither modal damping nor Rayleigh damping can model actual structural damping exactly and because modal damping requires more unknowns than the Rayleigh damping in the parameter estimation, the current formulation employs the Rayleigh damping for SI. The Rayleigh damping yields a linear fit to the actual damping of a structure. In case more accurate estimation of the actual damping is required, the Caughey damping model [15], which is the general form of the Rayleigh damping, may be adopted.

3. Time discretization and sensitivity

The objective function in Eq. (4) is discretized with respect to time as follows.

$$\begin{aligned}\Pi(\mathbf{x}(\tau),\tau) &= \frac{1}{2}\int_0^\tau \|\tilde{\mathbf{a}}(\mathbf{x}(\tau),t)-\bar{\mathbf{a}}(t)\|^2\,\mathrm{d}t + \frac{\lambda^2}{2}\int_0^\tau \left\|\frac{\mathrm{d}\mathbf{x}}{\mathrm{d}t}\right\|^2 \mathrm{d}t \\ &\approx \frac{1}{2}\sum_{k=1}^{nt}\|\tilde{\mathbf{a}}_k(\mathbf{x}_{nt})-\bar{\mathbf{a}}_k\|^2\Delta t + \frac{\lambda^2}{2}\sum_{k=1}^{nt}\frac{\|\mathbf{x}_k-\mathbf{x}_{k-1}\|^2}{\Delta t} \\ &= \frac{1}{2}\sum_{k=1}^{nt}\|\tilde{\mathbf{a}}_k(\mathbf{x}_{nt})-\bar{\mathbf{a}}_k\|^2\Delta t + \frac{\lambda^2}{2}\sum_{k=1}^{nt-1}\frac{\|\mathbf{x}_k-\mathbf{x}_{k-1}\|^2}{\Delta t} + \frac{\lambda^2}{2}\frac{\|\mathbf{x}_{nt}-\mathbf{x}_{nt-1}\|^2}{\Delta t},\end{aligned} \tag{8}$$

where nt represents the number of time steps corresponding to current time $\tau = nt \times \Delta t$ and the subscript denotes time step. The definitions of the discretized variables used in Eq. (8) are

$$\tilde{\mathbf{a}}_k(\mathbf{x}_{nt}) = \tilde{\mathbf{a}}(\mathbf{x}(\tau), k\Delta t), \qquad \bar{\mathbf{a}}_k = \bar{\mathbf{a}}(k\Delta t), \qquad \mathbf{x}_k = \mathbf{x}(k\Delta t), \tag{9}$$

where $\mathbf{x}_0$ represents the initial values of the system parameters. Since the system parameters identified at the previous time steps are included in Eq. (8), the SI procedure should be performed sequentially for every time step in the interval of $0<\tau\leqslant\tau_{\max}$, where $\tau_{\max}$ is the final time for SI. The system parameters of the previous time steps are known and have no effect on the solution of the minimization problem for the current time step, and thus the second term of the last equation in Eq. (8) is omitted from the objective function. The final discretized minimization problem at time τ is written as follows.

$$\underset{\mathbf{x}_{nt}}{\mathrm{Min}}\ \Pi(\mathbf{x}_{nt},\tau) = \frac{1}{2}\sum_{k=1}^{nt}\|\tilde{\mathbf{a}}_k(\mathbf{x}_{nt})-\bar{\mathbf{a}}_k\|^2\Delta t + \frac{\lambda^2}{2}\frac{\|\mathbf{x}_{nt}-\mathbf{x}_{nt-1}\|^2}{\Delta t} \quad \text{subject to } \mathbf{r}(\mathbf{x}_{nt})\leqslant 0. \tag{10}$$

Since the minimization problem (10) is nonlinear with respect to the system parameters at time τ, the recursive quadratic programming (RQP) with the Fletcher active set strategy [17] is utilized. A line search technique is employed to accelerate convergence. The quadratic sub-problem of (10) for the RQP is defined as

$$\begin{aligned}\underset{\Delta\mathbf{x}_{nt}}{\mathrm{Min}}\ &\frac{1}{2}\Delta\mathbf{x}_{nt}\left(\mathbf{H}+\frac{\lambda^2}{\Delta t}\mathbf{I}\right)\Delta\mathbf{x}_{nt} + \Delta\mathbf{x}_{nt}\sum_{k=1}^{nt}\nabla_{\mathbf{x}}\tilde{\mathbf{a}}_k(\bar{\mathbf{x}}_{nt})\cdot(\tilde{\mathbf{a}}_k(\bar{\mathbf{x}}_{nt})-\bar{\mathbf{a}}_k)\Delta t \\ &+\frac{\lambda^2}{\Delta t}\Delta\mathbf{x}_{nt}\cdot(\bar{\mathbf{x}}_{nt}-\mathbf{x}_{nt-1}) \quad \text{subject to } \mathbf{r}(\bar{\mathbf{x}}_{nt}+\Delta\mathbf{x}_{nt})\leqslant 0,\end{aligned} \tag{11}$$

where $\mathbf{H}$ and $\nabla_{\mathbf{x}}$ are the Gauss–Newton Hessian matrix of the error function and the gradient operator with respect to the system parameters, respectively, and $\Delta\mathbf{x}_{nt}$ and $\bar{\mathbf{x}}_{nt}$ are defined as follows.

$$\Delta\mathbf{x}_{nt} = \mathbf{x}_{nt}^{j} - \mathbf{x}_{nt}^{j-1}, \qquad \bar{\mathbf{x}}_{nt} = \mathbf{x}_{nt}^{j-1}. \tag{12}$$

Here, the superscript j denotes the iterational count for the current time step nt. The Gauss–Newton Hessian matrix is defined as follows.

$$\mathbf{H} = \sum_{k=1}^{nt} \nabla_{\mathbf{x}} \tilde{\mathbf{a}}_k(\bar{\mathbf{x}}_{nt}) \cdot \nabla_{\mathbf{x}} \tilde{\mathbf{a}}_k(\bar{\mathbf{x}}_{nt}) \Delta t. \tag{13}$$

The Newmark-β method is employed to obtain the acceleration and its sensitivity at each time step. The displacement and the velocity for the kth time step are expressed in terms of acceleration as follows.

$$\begin{aligned} \mathbf{v}_k(\bar{\mathbf{x}}_{nt}) &= \mathbf{v}_{k-1}(\bar{\mathbf{x}}_{nt}) + \Delta t((1-\gamma)\mathbf{a}_{k-1}(\bar{\mathbf{x}}_{nt}) + \gamma \mathbf{a}_k(\bar{\mathbf{x}}_{nt})), \\ \mathbf{u}_k(\bar{\mathbf{x}}_{nt}) &= \mathbf{u}_{k-1}(\bar{\mathbf{x}}_{nt}) + \mathbf{v}_{k-1}(\bar{\mathbf{x}}_{nt})\Delta t + \frac{(\Delta t)^2}{2}((1-2\beta)\mathbf{a}_{k-1}(\bar{\mathbf{x}}_{nt}) + 2\beta \mathbf{a}_k(\bar{\mathbf{x}}_{nt})), \end{aligned} \tag{14}$$

where β and γ are the integration constants of the Newmark β-method. Substitution of Eq. (14) into the equation of motion (1) yields the following well-known expression for the acceleration of a structure:

$$\mathbf{a}_k(\bar{\mathbf{x}}_{nt}) = (\hat{\mathbf{M}}_k(\bar{\mathbf{x}}_{nt}))^{-1} \hat{\mathbf{P}}_k(\bar{\mathbf{x}}_{nt}), \tag{15}$$

where

$$\begin{aligned} \hat{\mathbf{M}}_k(\bar{\mathbf{x}}_{nt}) &= \mathbf{M} + \gamma \Delta t \mathbf{C}(\bar{\mathbf{x}}_{nt}) + \beta(\Delta t)^2 \mathbf{K}(\bar{\mathbf{x}}_{nt}), \\ \hat{\mathbf{P}}_k(\bar{\mathbf{x}}_{nt}) &= \mathbf{p}_k - \mathbf{C}(\bar{\mathbf{x}}_{nt})(\mathbf{v}_{k-1}(\bar{\mathbf{x}}_{nt}) + \Delta t(1-\gamma)\mathbf{a}_{k-1}(\bar{\mathbf{x}}_{nt})) \\ &\quad - \mathbf{K}(\bar{\mathbf{x}}_{nt})\left(\mathbf{u}_{k-1}(\bar{\mathbf{x}}_{nt}) + \Delta t \mathbf{v}_{k-1}(\bar{\mathbf{x}}_{nt}) + \frac{(\Delta t)^2}{2}(1-2\beta)\mathbf{a}_{k-1}(\bar{\mathbf{x}}_{nt})\right). \end{aligned} \tag{16}$$

The sensitivity of acceleration is obtained by the direct differentiation of Eq. (15).

$$\frac{\partial \mathbf{a}_k}{\partial x_{nt}^i} = (\hat{\mathbf{M}}_k)^{-1}\left(\frac{\partial \hat{\mathbf{P}}_k}{\partial x_{nt}^i} - \frac{\partial \hat{\mathbf{M}}_k}{\partial x_{nt}^i}\mathbf{a}_k\right), \tag{17}$$

where x_{nt}^i is the ith component of system parameter vector at time τ, $\mathbf{x}_{nt}$. Once the sensitivity of acceleration is calculated, the sensitivities of displacement and velocity are easily evaluated by the direct differentiation of Eq. (14) with respect to the system parameters. The sensitivities of the initial conditions usually vanish since the initial conditions are independent of the system parameters. In case, however, a structure is suddenly released from a static equilibrium state, the sensitivity of the initial displacement to the stiffness parameters exists, and thus the sensitivity of initial velocity has a non-zero value. In this case, the sensitivity of initial displacement is obtained by the direct differential of the static equilibrium equation.

4. Validations of the proposed algorithm

The validity of the proposed time-domain SI is demonstrated through a numerical simulation study for a two-span continuous truss and a laboratory experimental study for a three story shear

building. The integration constants of the Newmark β-method, $\beta = \frac{1}{2}$, $\gamma = \frac{1}{4}$, are used for all cases. The regularization factor is calculated by the GMS.

4.1. Numerical simulation study

A two-span continuous planar truss used in this numerical simulation study is shown in Fig. 2. The axial rigidity of each member and the Rayleigh damping coefficients are selected as the system parameters. The material property is selected as typical steel (Young's modulus = 210 GPa, specific mass = 7850 kg/m^3). The initial cross sectional areas of top, bottom, vertical, and diagonal members of the truss are 250, 300, 200, and 220 cm^2, respectively. Damage of the truss is implemented as 40%, 50%, and 55% reductions in the sectional areas of member 7, 16, and 31, respectively. The damaged members are depicted as dotted lines in Fig. 2. The computed natural frequencies of the undamaged truss range from 6.6 Hz for the lowest mode to 114.7 Hz for the highest mode.

A free vibration is induced by a sudden release of applied loads of 50 KN at the mid-spans as shown in Fig. 2 from the static equilibrium. The measured accelerations are obtained by adding 8% random noise generated from a uniform probability function to acceleration calculated by the finite element analysis unless otherwise stated. The uniform probability function is selected to generate to random noise because it generates more widely distributed errors than the normal distribution for the given amplitude of noise. The observation points are located at 12 bottom nodes of the truss, which are depicted as solid circles in Fig. 2. Acceleration is measured in the time period from 0 to 1.0 s with the interval of $\frac{1}{200}$ s. Horizontal accelerations are measured at the two observation points located at the roller supports while vertical accelerations are measured at the other observation points. Modal damping is employed for simulating measured acceleration while the Rayleigh damping is adopted for the SI. The modal damping ratios used to simulate measured acceleration are shown in Fig. 8, in which the modal damping ratios vary continuously from 3% for the first mode to 30% for the last mode. The initial values of the Rayleigh damping coefficients, a_0 and a_1 are assumed as 2.32 and 1.05×10^{-3}, respectively, and the initial modal damping ratios calculated by Eq. (7) are also shown in Fig. 8.

The developed time-domain SI algorithm is applied to estimate the system parameters of the damaged structure using acceleration measured for 1.0 s at the observation points. The total number of unknown parameters estimated is 57 including 55 member axial rigidities and two damping coefficients. The variations of axial rigidities of the damaged members and three typical

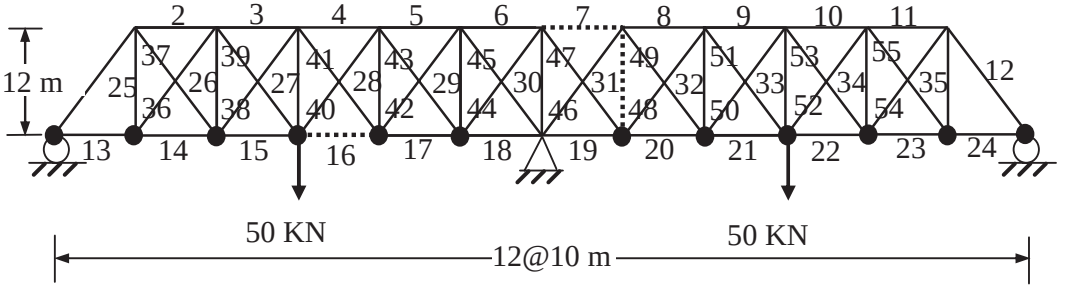

Fig. 2. Two-span continuous truss.

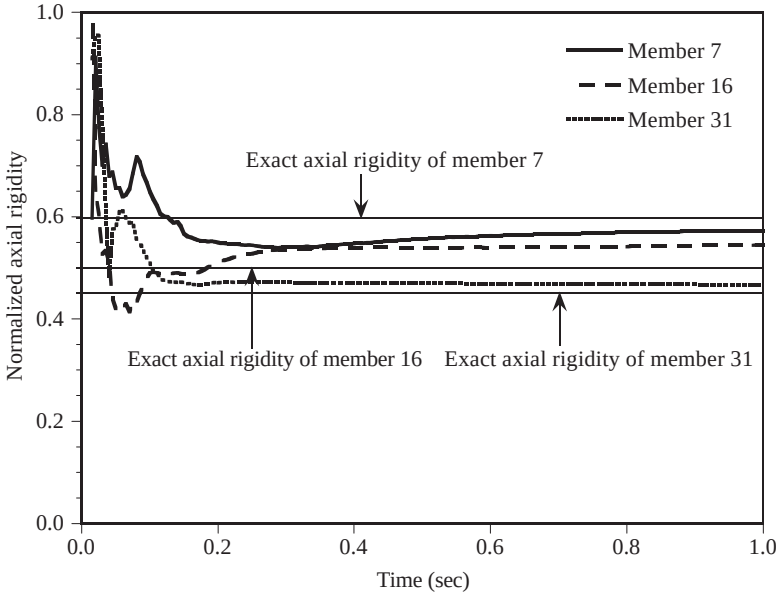

Fig. 3. Variation of axial rigidities of damaged members.

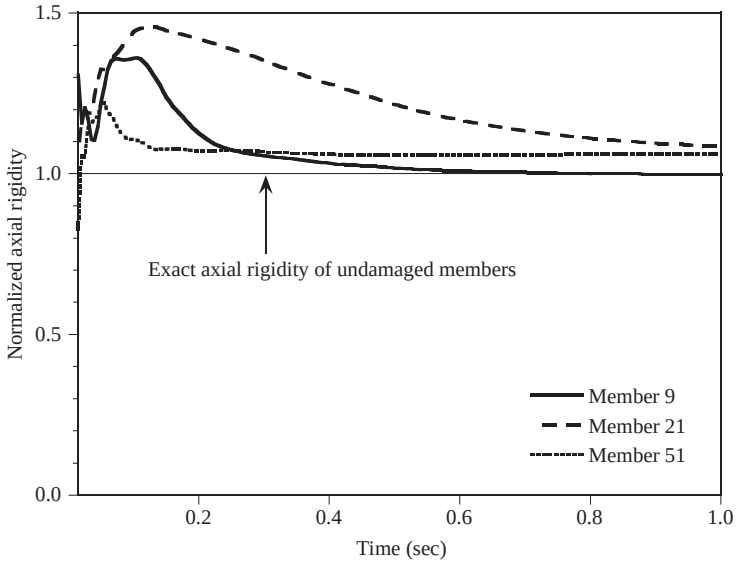

Fig. 4. Variation of axial rigidities of typical undamaged members in the right span.

undamaged members in the right span are drawn with respect to time in Figs. 3 and 4, respectively. From the figures, it is clearly seen that the estimated stiffness parameters of damaged members converge to the actual values as time steps proceed. Fig. 5 shows the axial rigidity of

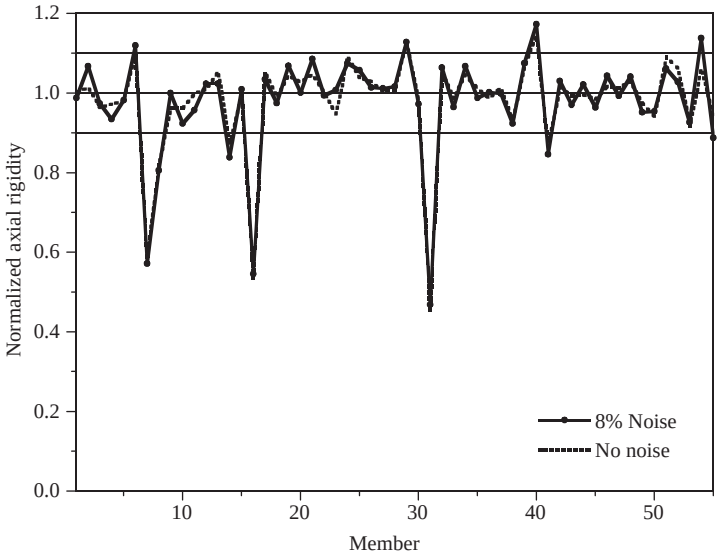

Fig. 5. Identified axial rigidities at the final time step, $\tau = 1.0$ s.

each member identified at the final time $\tau = 1.0$ s. The vertical axes of Figs. 3–5 represent the normalized axial rigidity with respect to the initial value of each member. The proposed SI scheme identifies the damaged members and their damage severity quite accurately. The identified axial rigidities oscillate moderately within the range of $\pm 10\%$ for 44 undamaged members out of 52 while the oscillation magnitudes of the other eight undamaged members are a little higher than 10%. Since, however, axial rigidities of the damaged members are reduced prominently compared with those of the other members, the damaged members are clearly distinguished from undamaged members. The identified axial rigidities with noiseless acceleration data, which represent the most accurate and stable solution for this example, are shown in Fig. 5 as a dotted line. Although there is no noise in measurement, the identified stiffness properties oscillate because of the modeling error [4] in damping. The noisy data and the noiseless data yield almost identical results, which demonstrates the robustness of the proposed method to measurement noise. Fig. 6 compares the measured acceleration with the calculated acceleration at the middle of the left span by the identified system parameters at the final time step. The root mean square error of the calculated acceleration to the measured acceleration is evaluated as 6.3%. The calculated acceleration agrees well with the measured one.

Fig. 7 shows the variations of Rayleigh damping coefficients in time. The coefficients for the mass and the stiffness are drawn against the left and the right vertical axis, respectively. The damping coefficients converge slower than the stiffness properties. The ratio of the Frobenius norm [16] of the stiffness term to that of the mass term in the damping matrix is calculated as 32.4, which means that a_1 plays a much more important role than a_0 in the damping matrix. The Frobenius norm of a matrix is defined as the square root of the sum of the squares of all elements in the given matrix. Fig. 8 shows the variations of damping ratios calculated by Eq. (7) with frequency at the final time step. The identified Rayleigh damping approximates the exact modal

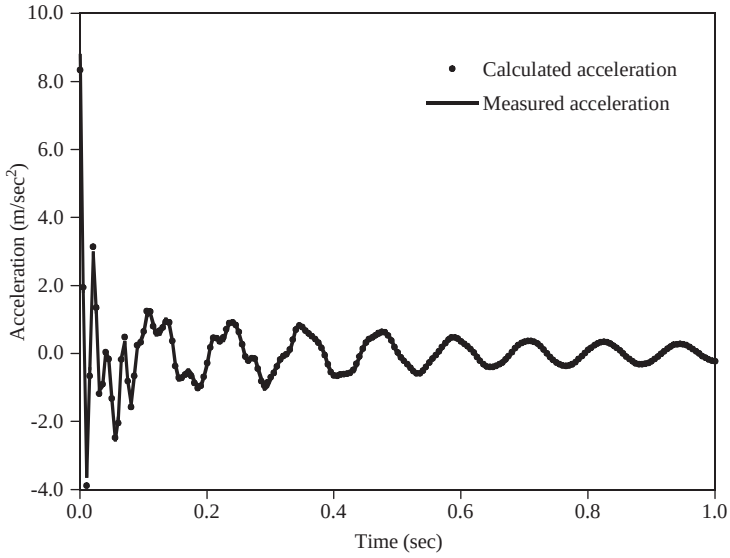

Fig. 6. Measured and calculated acceleration at the center of the left span.

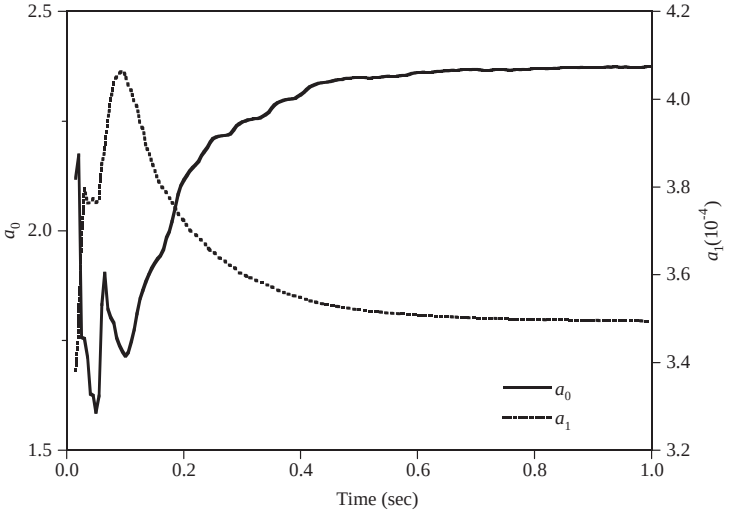

Fig. 7. Variation of Rayleigh damping coefficients.

damping closely in the range up to 60 Hz, which corresponds to the 22nd mode, while the errors in the modal damping ratios become larger for higher modes. Since, however, the natural frequencies corresponding to dominant lower modes are much less than 60 Hz, such approximation is good enough to identify the system parameters and to match the dynamic response correctly.

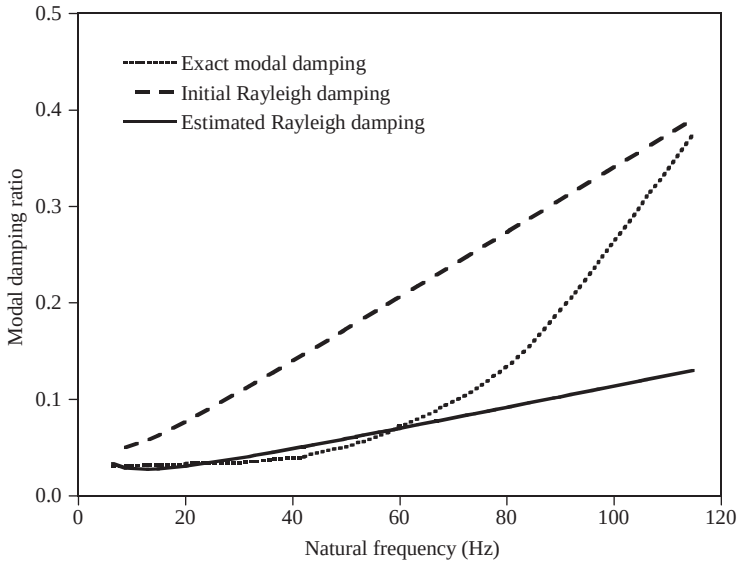

Fig. 8. Identified modal damping ratios at the final time step, $\tau = 1.0\,\mathrm{s}$.

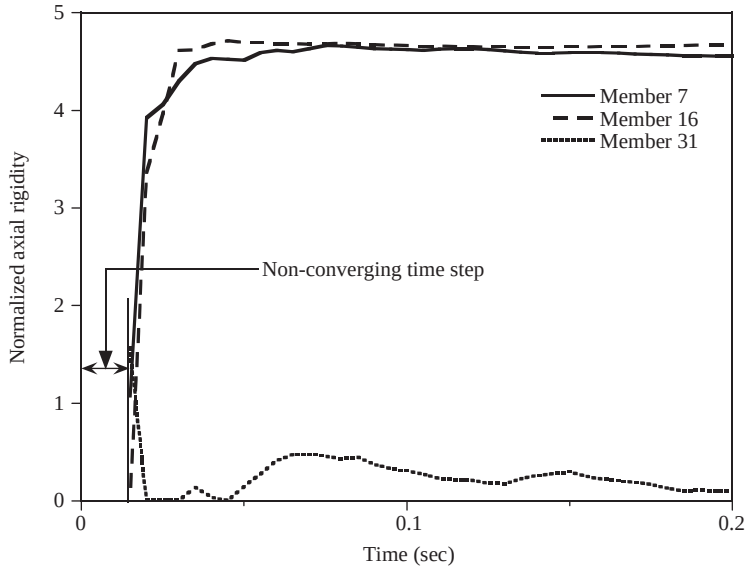

Fig. 9. Variation axial rigidities of damaged members without damping estimation.

Fig. 9 shows the variation of the identified axial rigidities of the damaged members with time in case the Rayleigh damping coefficients are fixed at their initial values without being estimated. As shown in the figure, the solution converges to totally meaningless values. At the earlier time steps,

the optimization procedure does not converge even after 30 iterations. Since the identified axial rigidities at the final step oscillate too severely, the results are not presented. This oscillation occurs because the energy dissipation caused by damping cannot be modeled properly by merely adjusting the stiffness parameters of a structure without allowing the correction of damping characteristics. Therefore, the damping characteristics should be estimated through SI procedure in case the accurate damping characteristics are not known a priori, which is true for actual situations.

4.2. Experimental study

An experimental laboratory study is carried to verify the developed time-domain SI algorithm. A three-story shear-building model and its numerical model are shown in Figs. 10 and 11, respectively. The floor plate, which is supported by four steel columns, consists of a 45 cm × 45 cm rectangular steel plate welded to 5 mm plates on all four sides to increase the flexural stiffness and

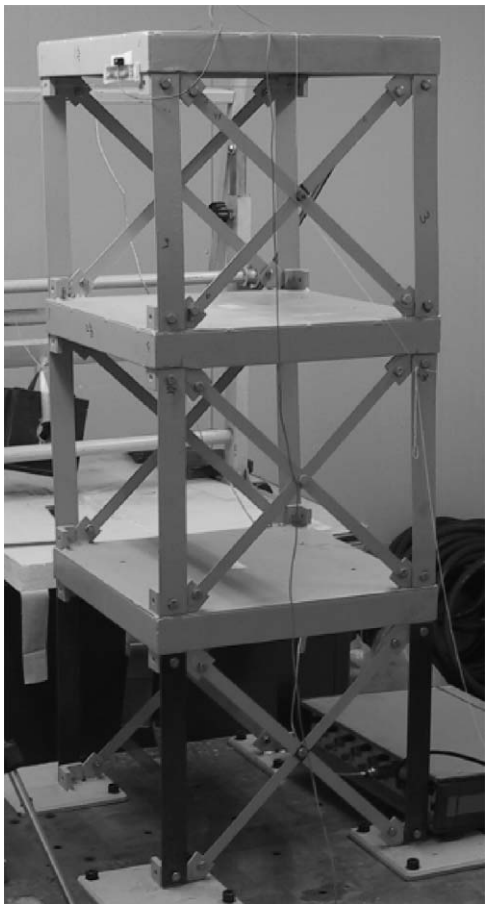

Fig. 10. Three-story shear building model.

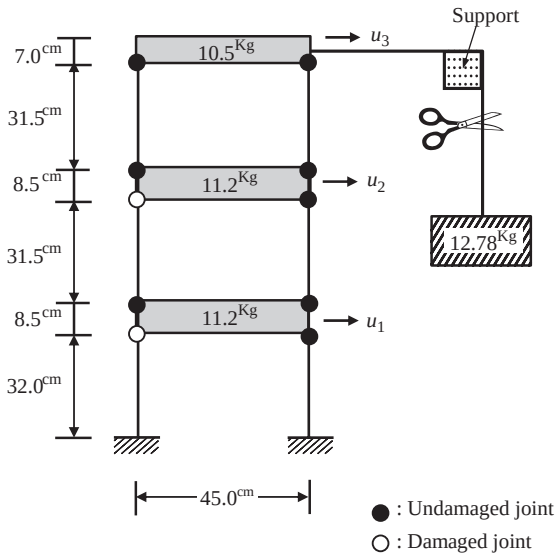

Fig. 11. Numerical model of the three-story shear building and the initial loading condition.

Table 1
Cross sectional properties and flexural rigidities of columns

Column	Thickness (cm)	Area (cm^2)	Mass (g)	EI (N-m^2)
1st story	0.3	1.2	1196	75.6
2nd story	0.2	0.8	868	22.4
3rd story	0.2	0.8	870	22.4

to connect the floor plate to the columns. A column in each story is connected to the bottom and upper floor plates by a bolt independently of the columns of the other story. Two sets of cross bracings are installed in the plane perpendicular to the plane of vibration to prevent out-of-plane vibrations in each story.

The cross sectional properties, weights and flexural rigidities of the columns are given in Table 1. In the table, the cross sectional properties are for one column, while the weight and the flexural rigidity represent the sum of four columns in each story. The dimension and weight of each column and floor plate are measured with calipers and a scale. The Young's modulus of each column is not measured through a material test, and is assumed as a representative value of steel, 210 GPa. The flexural rigidity of each story in Table 1 is a calculated rigidity by the measured dimensions of a column and the assumed Young's modulus, and is referred to as the measured flexural rigidity hereafter. Each column is modeled by two beam elements for an accurate dynamic analysis, and thus there are nine dof in the numerical model. The natural frequencies for the horizontal modes of the finite element model with the properties summarized in Table 1 are 2.43, 6.58 and 9.26 Hz.

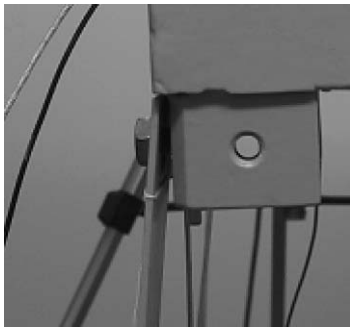

Fig. 12. Close look of a damaged joint.

Accelerometers are placed horizontally in the plane of vibration at the center of each floor plate, and time histories of accelerations are measured at the sampling rate of 50 Hz for 200 s and the measured accelerations during the first 40 s are used for the identification. Free vibration is induced by the sudden release of a hanging steel block of 12.78 kg as shown in Fig. 11. Due to friction between the support and the cable hanging the weight, 104.5 N (83.4% of the total weight) is applied to the structure, which is measured by a load cell.

The proposed SI is applied for the intact structure and a damaged structure. Damage of the shear building is introduced by loosening two bolts out of four at the joints between the columns and the floor plate at the 1st and 2nd floor as shown in Fig. 12. Two bolts are loosened at the top of the two columns in the 1st and the 2nd story, while the bolts at the bottom of the columns in the stories are fixed as the intact state. Therefore, the columns with loosened bolts behave like fixed-hinged beams. The flexural rigidity of each story and the two Rayleigh damping coefficients are the system parameters to be estimated for this example. The measured flexural rigidities shown in Table 1 are used as the initial flexural rigidities of the intact structure for SI while the flexural rigidities identified for the intact structure are taken as the initial values of the damaged structure. Three measurement cases are tried for the damaged structure. The acceleration data measured at all floors, the 2nd and the 3rd floor, and only the 3rd floor are used in measurement cases I, II, and III, respectively. Only measurement case I, which is believed to yield the most accurate results, is tried for the intact structure.

Fig. 13 shows the measured accelerations at the 3rd floor for the intact structure and the damaged structure. The decrease in the natural frequency due to damage is clearly noticeable. Since the loosened joints act like hinges rather than fixed joints, the reduction of the total flexural stiffness of the four columns with the loosened bolts is approximately estimated as 62.5% of their original stiffness by an elementary calculation of structural analysis.

$$\frac{2 \times 12EI/l + 2 \times 3EI/l}{4 \times 12EI/l} \times 100 = 62.5\%. \tag{18}$$

The variation of identified flexural rigidity of each story for measurement case I is shown in Figs. 14 and 15 for the intact structure and the damaged structure, respectively. The flexural rigidities converge very fast in both cases. Table 2 shows the identified flexural rigidities. For the intact structure, the identified flexural rigidity of the 1st and the 3rd story increase by 35% and

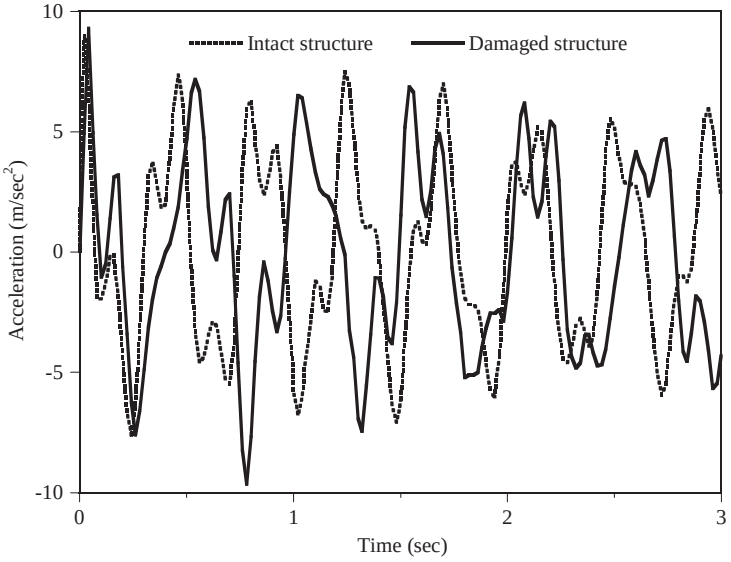

Fig. 13. Time history of acceleration of the three story shear building.

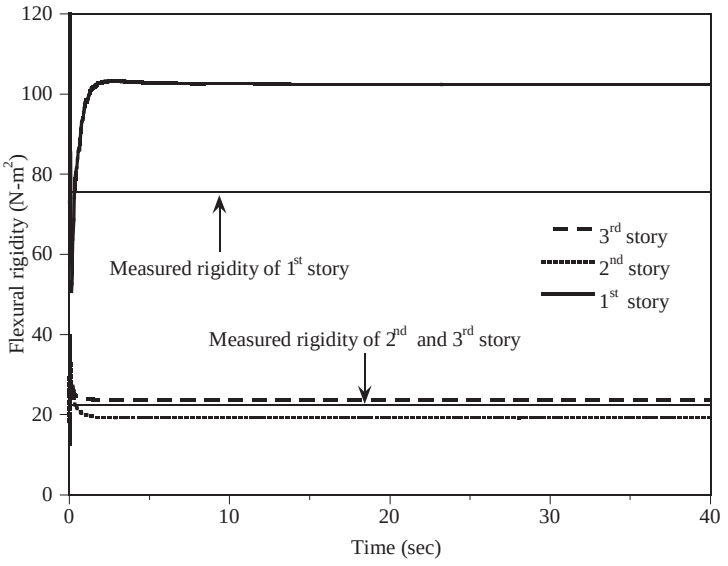

Fig. 14. Variation of flexural rigidities in the intact structure.

5.8%, respectively, while that of the 2nd floor decreases by 13.4% from their initial values. It seems that the changes in the flexual rigidities from the measured values are mainly caused by the damping characteristics of the frame since the natural frequencies do not change much compared to the identified damping ratios in Table 4. Especially, the flexural rigidity of the 1st story, which has the lowest sensitivity to the frequency of the dominant first mode, changes most to model a proper damping ratio of each mode without affecting the natural frequency.

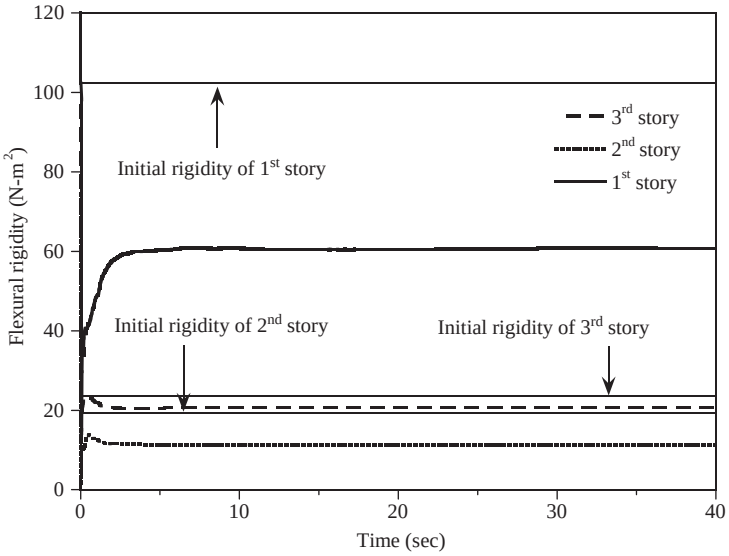

Fig. 15. Variation of flexural rigidities in the damaged structure.

Table 2
Identified flexural rigidity of each story (Unit: N – m^2)

Column	Measured	Intact (Case I)	Damaged (Case I)	Damaged (Case II)	Damaged (Case III)
1st story	75.6	102.4	60.8	60.3	75.3
2nd story	22.4	19.4	11.3	11.3	10.9
3rd story	22.4	23.7	20.7	20.7	20.1

The damage status should be determined based on the identified stiffness parameters of the intact structure since the stiffness parameters may vary to model the actual damping characteristics by the Rayleigh damping regardless of the damage status of the frame. Damage due to the loosened bolt at the 1st and 2nd floors is clearly assured by comparing Fig. 14 with Fig. 15. For the damaged structure, the flexural rigidities of the 1st and the 2nd story decrease to 58% and 59% of the identified values for the intact structure, respectively, for measurement cases I and II, which are very close to the expected stiffness reduction given in Eq. (18). The damage of the 1st story seems to be underestimated for measurement case III. Nevertheless, the proposed method yields consistent results for the damaged structure in all measurement cases.

Table 3 shows the measured and identified natural frequencies. The measured natural frequencies are obtained by FFT using the measured acceleration data at the 3rd floor, while the identified natural frequencies are calculated by the eigenvalue analysis of the structure with identified system parameters. The identified frequencies for all cases agree very well with the measured natural frequencies. The natural frequencies decrease in the damaged structure for all modes. The identified modal damping ratios are shown in Table 4. The damping ratios increase in the damaged structure for all modes, and identified results are consistent in all measurement cases.

Table 3
Identified natural frequency (Unit: Hz)

Mode	Measured[a]		Identified			
	Intact	Damaged	Intact (Case I)	Damaged (Case I)	Damaged (Case II)	Damaged (Case III)
1st	2.39	1.88	2.40	1.89	1.89	1.89
2nd	6.48	5.93	6.86	6.18	6.18	6.18
3rd	8.95	7.28	10.01	7.77	7.75	8.36

[a]Calculated by FFT using the acceleration data at the 3rd floor.

Table 4
Initial and identified modal damping ratio (Unit: %)

Mode	Initial	Intact (Case I)	Damaged (Case I)	Damaged (Case II)	Damaged (Case III)
1st	1.2	0.44	0.45	0.47	0.47
2nd	3.1	0.67	0.87	1.11	0.98
3rd	4.7	0.91	1.07	1.35	1.29

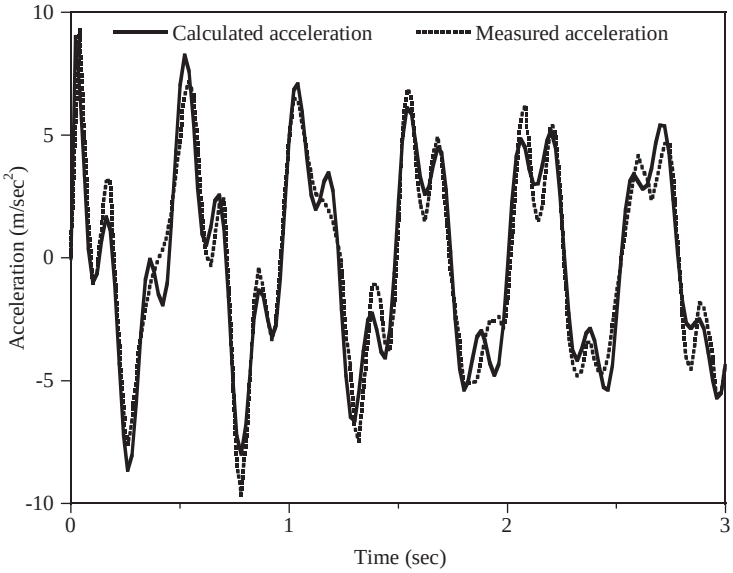

Fig. 16. Measured and calculated acceleration at the 3rd floor of the damaged structure.

It is believed that the impact between the columns and side plates of the 1st and 2nd floor during the dynamic motion of the damaged structure increases the rate of energy dissipation. The calculated acceleration using the converged system parameters at the final time step is compared with the measured acceleration at the 3rd floor for the damaged structure in Fig. 16. Since the

calculated and measured accelerations agree well each other in an overall sense, it is concluded that the system parameters estimated by the proposed method represent the actual status of the structure closely.

5. Conclusion

A time-domain SI using measured acceleration data is proposed. The system parameters include the damping parameters as well as the stiffness parameters of a structure. The Rayleigh damping is used to estimate the damping characteristics of a structure. The time integral of the least-squared errors between calculated acceleration and measured acceleration is adopted as an error function. The regularization technique is employed to alleviate the ill-posedness of the inverse problem in SI. A new regularization function is proposed for the time-domain SI. The GMS is utilized to determine the optimal regularization factor.

It is confirmed that the damping characteristics should be adjusted properly according to measured acceleration data, and that a meaningless solution may be obtained without proper estimation of damping characteristics. Although it is not possible to form the exact damping matrix of a structure, it is very important to approximate the damping parameters to the real damping as closely as possible. The proposed method is able to estimate the stiffness properties accurately even though the damping characteristics are approximated by the Rayleigh damping. The proposed method yields accurate and stable solutions for numerically generated data and the experimentally measured data.

This paper focuses on developing a time-domain SI algorithm rather than a damage detection scheme. Since SI problems are ill-posed and their solutions are very sensitive to noise components in measurement, a reliable damage detection algorithm requires further development based on the proposed SI algorithm. It is believed the proposed method provides a very powerful engineering tool to identify dynamic characteristics of structures, and provides a fundamental SI algorithm to implement a reliable damage detection scheme in structures using measured accelerations.

Acknowledgements

This work was supported by the Korea Science and Engineering Foundation (KOSEF) through the Korea Earthquake Engineering Research Center at Seoul National University. The authors are very grateful to Prof. H. M. Koh of Seoul National University, Seoul, Korea for allowing them to use the shear building model.

References

[1] K.D. Hjelmstad, S. Shin, Damage detection and assessment of structures from static response, *Journal of Engineering Mechanics* 123 (6) (1997) 568–576.

[2] H.S. Lee, Y.H. Kim, C.J. Park, H.W. Park, A new spatial regularization scheme for the identification of the geometric shape of an inclusion in a finite body, *International Journal for Numerical Methods in Engineering* 46 (7) (1999) 973–992.

[3] I. Yeo, S. Shin, H.S. Lee, S.P. Chang, Statistical damage assessment of framed structures from static responses, *Journal of Engineering Mechanics* 126 (4) (2000) 414–421.
[4] H.W. Park, S. Shin, H.S. Lee, Determination of an optimal regularization factor in system identification with Tikhonov regularization for linear elastic continua, *International Journal for Numerical Methods in Engineering* 51 (10) (2001) 1211–1230.
[5] K.D. Hjelmstad, S. Shin, Crack identification in a cantilever beam from modal response, *Journal of Sound and Vibration* 198 (5) (1996) 527–545.
[6] Z.Y. Shi, S.S. Law, L.M. Zhang, Damage localization by directly using incomplete mode shapes, *Journal of Engineering Mechanics* 126 (6) (2000) 656–660.
[7] F. Vestroni, D. Capecchi, Damage detection in beam structures based on frequency measurements, *Journal of Engineering Mechanics* 126 (7) (2000) 761–768.
[8] K.D. Hjelmstad, M.R. Banan, M.R. Banan, Time-domain parameter estimation algorithm for structures I: computational aspects, *Journal of Engineering Mechanics* 121 (3) (1995) 424–434.
[9] M.R. Banan, M.R. Banan, K.D. Hjelmstad, Time-domain parameter estimation algorithm for structures II: numerical simulation studies, *Journal of Engineering Mechanics* 121 (3) (1995) 435–447.
[10] L. Ge, T.T. Soong, Damage identification through regularization method I: theory, *Journal of Engineering Mechanics* 124 (1) (1998) 103–108.
[11] C.-H. Huang, A non-linear inverse vibration problem of estimating the time-dependent stiffness coefficients by conjugate gradient method, *International Journal for Numerical Methods in Engineering* 50 (2001) 1545–1558.
[12] M. Raghavendrachar, A.E. Aktan, Flexibility by multireference impact testing for bridge diagnostics, *Journal of Structural Engineering* 118 (8) (1992) 2186–2203.
[13] H.D. Bui, *Inverse Problems in the Mechanics of Materials: an Introduction*, CRC Press, Boca Raton, 1994.
[14] P.C. Hansen, *Rank-deficient and Discrete Ill-posed Problems: Numerical Aspects of Linear Inversion*, SIAM, Philadelphia, 1998.
[15] A.K. Chopra, *Dynamics of Structures: Theory and Applications to Earthquake Engineering*, second ed., Prentice-Hall, Englewood Cliffs, NJ, 2001.
[16] G.H. Golub, C.F. Van Loan, *Matrix Computations*, third ed., Johns Hopkins University Press, Baltimore, 1996.
[17] D.G. Luenberger, *Linear and Nonlinear Programming*, second ed., Addison Wesley, Reading MA, 1989.